1.3 **Properties of Quasars**

By late 1964, Schmidt had studied a sufficient number of quasars to define their properties (Schmidt 1969):

- Star-like objects identified with radio sources.
- Time-variable continuum flux.
- Large UV flux.
- Broad emission lines.
- Large redshifts.

Not all objects that we now call AGNs share every one of these properties. In fact, the single most common characteristic of AGNs is probably that they are all luminous X-ray sources (Elvis *et al.* 1978). Nevertheless, the characteristics identified by Schmidt are important for understanding the physics of AGNs and as well as understanding the techniques by which AGNs are found. We will therefore discuss these various properties individually below.

In more modern terms, one of the defining characteristics of quasars is their very broad spectral energy distribution, or SED (Fig. 1.3). Quasars are among the most luminous objects in the sky at every wavelength at which they have been observed. Unlike spectra of stars or galaxies. AGN spectra cannot be described in terms of blackbody emission at a single temperature, or as a composite over a small range in temperature. Non-thermal processes, primarily incoherent synchrotron radiation, were thus invoked early on to explain quasar spectra.

In general, the broad-band SED of a quasar continuum can be characterized crudely as a power law

$$F_\nu = C\nu^{-\alpha}, \tag{1.5}$$

where a is the power-law index, *C* is a constant, and F_ν is the specific flux (i.e., per unit frequency interval), usually measured in units of ergs s^{-1} cm^{-2} Hz^{-1}. The convention that we adopt throughout this book is that a positive spectral index characterizes a source whose flux density *decreases* with increasing frequency. The reader is cautioned that some authors absorb the minus sign into the definition of the spectral index (e.g., $F_\nu = C\nu^{\alpha}$). Specific fluxes, particularly in the ultraviolet and optical parts of the spectrum, are often measured per unit wavelength interval (i.e., in units of ergs s^{-1} cm^{-2} A^{-1}) rather than per unit frequency interval. The total flux measured in any bandpass is the same, of course, whether the bandwidth is measured in frequency or in wavelength, so the relationship $F_\nu d\nu = F_\lambda d\lambda$ always holds. The transformation between the two systems is thus

$$F_\nu = F_\lambda \left|\frac{d\lambda}{d\nu}\right| = \frac{\lambda^2 F_\lambda}{c}, \tag{1.6}$$

so an equivalent form to eq. (1.5) is $F_\lambda = C'\lambda^{-2}$.

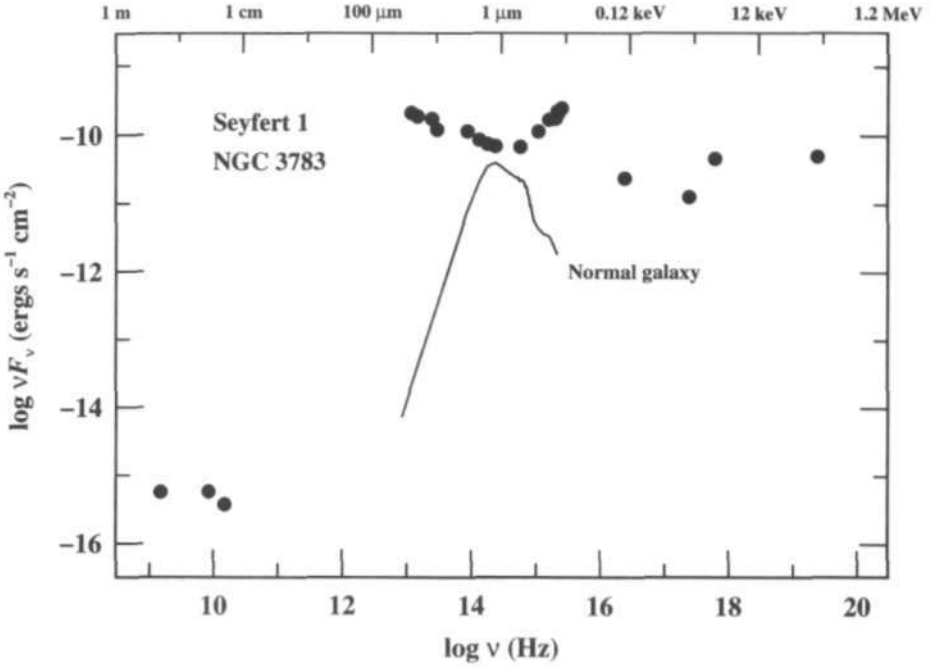

Fig. 1.3. The spectral energy distribution (SED) of the Seyfert 1 galaxy NGC 3783 (Alloin *et al*. 1995), from radio to y-ray energies. Shown for comparison is SED for a normal (type Sbc) galaxy, from a template spectrum compiled by Elvis *et al*. (1994). The flux scale of the normal galaxy spectrum has been adjusted to give the correct relative contribution of AGN component and starlight for NGC 3783 (in mid-1992) at 5125 A through a 5" x 10" spectrograph aperture.

Fits to quasar spectra over large frequency ranges yield spectral indices that are typically in the range O i a ^ 1, but different values of a are found for different spectral ranges. Indeed, it is obvious that a single power law cannot hold over all frequencies as the integrated power would diverge either at high frequencies (for a < 1) or at low frequencies (for a > 1). Over a frequency range vi — vi, the total power received is

$$\begin{aligned} P(\nu_1,\nu_2) &= \int_{\nu_1}^{\nu_2} F_\nu d\nu = C\int_{\nu_1}^{\nu_2} \nu^{-\alpha} d\nu \\ &= \frac{C}{1-\alpha}\left(\nu_2^{1-\alpha}-\nu_1^{1-\alpha}\right) \quad (\alpha \neq 1) \\ &= C \ln\left(\frac{\nu_2}{\nu_1}\right) \qquad (\alpha = 1). \end{aligned} \tag{1.7}$$

The case a = 0, a 'flat spectrum' on a conventional plot of specific flux versus frequency, has equal energy per unit frequency interval and the case a = 1 has equal energy per

unit *logarithmic* frequency interval.† A useful way to plot the broad-band SED in quasars is on a logνF_ν. versus logν diagram, as in Fig. 1.3. In this case, the power-law distribution becomes νF_ν oc $\nu^{1-\alpha}$, so the case $\alpha = 1$ is a horizontal line in such a diagram, and the $\alpha = 0$ spectrum rises with frequency. This is the preferred format for examining where the quasar energy is actually emitted as it reflects the amount of energy emitted in each equally spaced interval on the logarithmic frequency axis.

1.3.1 Radio Properties of Quasars

The radio morphology of quasars and radio galaxies is often described broadly in terms of two components, 'extended' (i.e., spatially resolved) and 'compact' (i.e., unresolved at ~1" resolution), that have different spectral characteristics, although the synchrotron mechanism seems to be at work in both cases. The extended-component morphology is generally double, i.e., with two 'lobes' of radio emission more or less symmetrically located on either side of the optical quasar or center of the galaxy. The linear extent of the extended sources can be as large as megaparsecs. The position of the optical quasar is often coincident with that of a compact radio source. The major difference between the extended and compact components is that the extended component is optically thin to its own radio-energy synchrotron emission, whereas this is not true for the compact sources.

Although a detailed discussion of synchrotron radiation is beyond the scope of this book, we will summarize some of the basic properties of synchrotron-emitting sources. For a homogeneous source with constant magnetic field B, a power-law continuum spectrum (eq. 1.5) can be generated by the synchrotron mechanism by an initial power-law distribution of electron energies £ of the form

$$N(E)\,dE = N_0\,E^{-s}\,dE,$$

where $\alpha = (s - 1)/2$. For the extended component, a typical observed value of the power-law index is $\alpha \approx 0.7$, so $s \approx 2.4$. This applies at higher frequencies where synchrotron self-absorption is not important. At lower frequencies, the emitting gas is optically thick and the the trend towards increasing flux with decreasing frequency turns over to yield F_ν oc $\nu^{5/2}$. The turn-over frequency increases with the density of relativistic electrons in the source, although it depends on other parameters as well. The relativistic particle densities in the extended radio components are low enough that they are optically thin even at very low radio frequencies (at least to the 3C frequency of 158 MHz). Radio spectra sometimes curve downward at higher frequencies (i.e.. α increases with ν). The basic reason for this is that electrons radiate at frequencies proportional to their energies £, and the *rate* at which they lose energy is proportional to £^{2}. Thus, the highest-energy electrons radiate away their energy the most rapidly.

† The case $\alpha = 1$ is sometimes described as having equal energy per decade (or octave), i.e.. over any factor of 10 (or two) in frequency.

features known as 'jets\t which are extended linear structures (Bridle and Perley 1984). An example of a jet is seen in the FR II source shown in Fig. 1.4. Jets appear to originate at the central compact source and lead out to the extended lobes. They often show bends or wiggles between the central source and the point where the jet appears to expand into the extended radio structure. The appearance of jets suggests that they transport energy and particles from the compact source to the extended regions. Jets often appear on only one side of the radio source, and in cases where jets are seen on both sides one side (the 'counter-jet') is much fainter than the other. The difference in brightness is thought to be primarily attributable to 'Doppler beaming' which preferentially enhances the surface brightness on the side that is approaching the observer.

Source: Peterson, B.M. (1977) An Introduction to Active Galactiv Nuclei, Cambridge University Press.